Topological phase transition in the ternary half-Heusler alloy ZrIrBi

C. K. Barman and Aftab Alam*
Department of Physics, Indian Institute of Technology, Bombay, Powai, Mumbai 400 076, India

(Received 27 October 2017; published 6 February 2018)

Half-Heusler alloys provide a new platform for deriving a host of topologically exotic compounds through the inherent flexibility of tuning their hybridization strength (via lattice parameters), spin-orbit strength, substitution/doping, etc. Using the first-principles calculation within the density functional theory, we explore the possibility of realizing a topological insulating phase in a new half-Heusler material ZrIrBi. We discovered three routes through which ZrIrBi can be transformed to exhibit a topological nontrivial phase. They are (i) a hydrostatic expansion by 1% causing a band inversion with zero gap, (ii) a uniaxial strain along (001) direction which opens a band gap while preserving the inverted band order, and (iii) substitution of 50% Bi by As and 50% Zr by Hf forming the compounds ZrIr($As_{0.5}Bi_{0.5}$) and ($Zr_{0.5}Hf_{0.5}$)IrBi again showing a topologically nontrivial band inversion. A definitive proof of the surface conduction in all three cases are done by simulating surface band structures. We report the formation energies and the phonon dispersion for the three cases to confirm the chemical and mechanical stability of the compounds.

DOI: 10.1103/PhysRevB.97.075302

I. INTRODUCTION

Topological insulators (TIs) [1–4] are a new class of materials which are distinguished from ordinary insulators by nontrivial band topology associated with bulk electronic structure. The nontrivial topology of the bulk band structures give rise to metallic surface states, which are topologically protected against time reversal symmetry (TRS). Due to their novel properties, the TIs have potential applications in spintronics, quantum computations [3,5], etc. The TI properties can simply be realized by a bulk band inversion mechanism owing to spin-orbit coupling (SOC) [1,2,5–9]. From the past few years, the discovery of new TIs pick up an immense surge and research interest in various fields such as physics, material science, electrical engineering, etc. The first three-dimensional (3D) topological insulators discovered were Bi-based binary compounds such as $Bi_{1-x}Sb_x$ [10] and Bi_2Se_3 [6,11,12]. Later on a few other class of compounds were also speculated to show TI properties. More recently, the search is extended to multicomponent compounds and ternary half-Heusler alloys (THH) emerge as a promising platform in realizing new 3D topological insulators. The much wider flexibility in design of Heusler compounds open up the possibility of tuning band gap and SOC. The importance of SOC is related to the presence of heavy elements in the concerned alloy. Apart from SOC, the external strain affects the hybridization strength, which in turn induces the topological phase transition originating from the critical response of valence and conduction bands.

Ternary Heusler alloys crystallizes in the space group $F\bar{4}3m(216)$ [13] which involved three interpenetrating fcc lattices. The chemical composition can be described by an XYZ formula, where X,Y are the transition or rare earth and Z is the main group elements. The Wyckoff positions of X, Y, and Z elements are 4b($\frac{1}{2}\frac{1}{2}\frac{1}{2}$), 4c($\frac{1}{4}\frac{1}{4}\frac{1}{4}$), and 4a(000) respectively. Typically an XYZ compound can be viewed as X^{n+} stuffing with zincblende type lattice $[YZ]^{n-}$. The crystal structure, in primitive cell, is shown in Fig. 1(a). Ternary Heusler compounds form a closed shell ($d^{10}s^2p^6$) structure with 18 valence electrons, exhibiting semiconducting properties.

In this article we investigated a new system ZrIrBi from the Heusler family which shows topological insulating behavior under strain (both hydrostatic as well as uniaxial). Nontrivial (topological) insulating properties are also realized by simple alloying of this compound with arsenic and bismuth. A careful study of the surface band structure, showing metallic nature, is also carried out. Sensitivity of surface properties with respect to various terminating layers is discussed in some detail. Chemical and mechanical stability of these compounds are confirmed from the calculated formation energy and the phonon dispersion. ZrIrBi is thus an important compound to be promoted as a potential topological insulator.

Computational details: Calculations were performed within the framework of density functional theory (DFT), implemented in the Vienna *ab initio* simulation package (VASP) [14–16]. We have employed Perdew-Burke-Ernzerhof (PBE) [15] within the generalized gradient approximation (GGA), to describe the exchange and correlation functionals. Plane wave energy cutoff of 500 eV were used. Total energy (force) was converged up to 10^{-6} eV/cell (0.001 eV/Å). A $2 \times 2 \times 2$ supercell of the primitive cell is used for the alloy calculation. Γ-centered K mesh of $16 \times 16 \times 16$ ($8 \times 8 \times 8$) points were used for bulk (supercell) Brillouin zone (BZ) integration. In addition, we have also performed the bulk calculations using hybrid functional (HSE-06) [17] to confirm the TI properties of the concerned compounds.

*aftab@iitb.ac.in

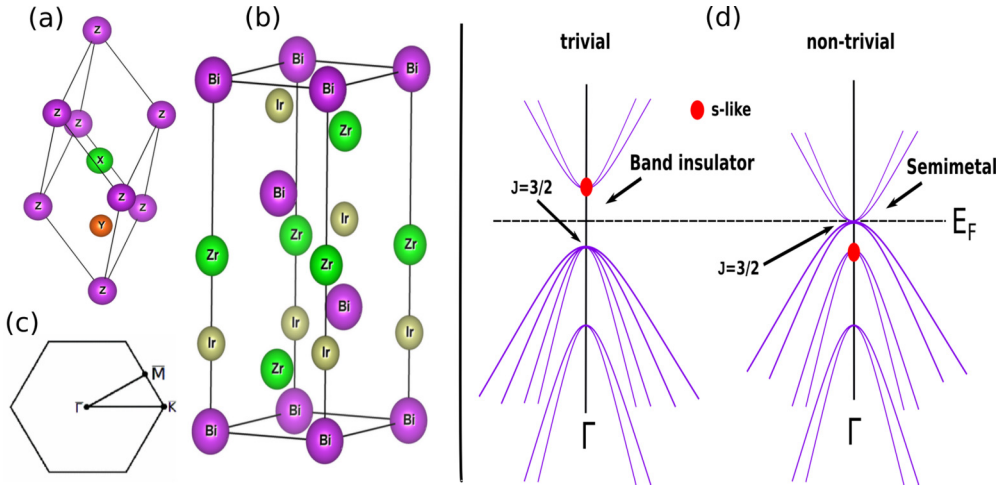

FIG. 1. (a) Primitive unit cell of a standard half-Heusler (XYZ) alloy. (b) Unit cell of ZrIrBi cleaved along the (111) surface. (c) Surface Brillouin zone (BZ) with high symmetry points. (d) Standard band structures for topologically trivial and nontrivial insulators near Γ point. Red dots indicate the s-like orbitals at Γ point. Band inversion occurs in the nontrivial case where s-like orbitals lie below the fourfold degenerate $J = \frac{3}{2}$ bands.

II. RESULTS AND DISCUSSIONS

Ternary half-Heusler (THH) compounds show close analogy with those of the well known HgTe and CdTe compounds. Topologically nontrivial HgTe [18] and trivial CdTe are two binary compounds both with zincblende structure which can be thought of as a half-Heusler alloy with vacant X site in the chemical description of THH (i.e., XYZ). HgTe [18] has a unique band structure, where two pairs of concave up (bottom of the conduction band) and concave down (top of the valence band) bands touching the Γ point are fourfold degenerate at Fermi level (E_F) making this compound nontrivial semimetallic. A schematic of such a band is shown in Fig. 1(d). These fourfold degenerate bands possess Γ_8 symmetry, exhibiting p-like orbital occupancy with total angular momentum $J = \frac{3}{2}$ and lies in energy above the twofold s-like pair Γ_6, representing an inversion order of band. Such band inversion is a strong indication of Z_2 topological insulators [6,7]. Whereas, in the case of CdTe, the s-like Γ_6 bands lie above the Γ_8 state, showing normal band ordering [18] [see Fig. 1(d)].

Band inversion in topological insulators is intimately tied to the nature of hybridization of adjacent atoms in the crystal. As such, external pressure can play an important role in inducing the nontrivial band topology in these classes of compounds. Chemical alloying (doping) is another interesting route to obtain band inversion and hence realize topological ordering.

In the following sections we will show how ZrIrBi transforms to a nontrivial insulator under the effect of hydrostatic as well as uniaxial strain. We will also show that alloying ZrIrBi with (i) Hf @ Ir site and (ii) As @ Bi site also induce band inversion, confirming the topological insulating behavior. Simulated band structure for (iii) surface will also be presented, which turns out to be metallic as expected.

A. Pristine ZrIrBi at ambient condition

Figure 2(b) shows the electronic structure of ZrIrBi at relaxed lattice parameter ($a_{\text{opt}} = 6.48$ Å), exhibiting a semiconducting gap 0.068 eV. The band topology of this system at ambient condition follows a normal band filling order similar to that of CdTe. In other words, the s/p band inversion, responsible for topological order, is absent here.

B. Topological phase transition (bulk)

1. Hydrostatic pressure

Next, we have analyzed the electronic structure of ZrIrBi under hydrostatic pressure. Figures 2(a) and 2(c) show the band structure under 1% uniform compression and expansion of the lattice with respect to a_{opt}, respectively. Upon 1% expansion, the system transforms to a zero-gap semimetal with fourfold degeneracy ($J = \frac{3}{2}$ states) at Γ point along with an inverted band order. This is obvious because the s-like band (red dots) lies below the $J = \frac{3}{2}$ states. Whereas the compression of the lattice [Fig. 2(a)] does not induce any topological phase transition and maintains the trivial band order with a slightly increased band gap. In order to check the strength of the nontrivial nature of the band insulator, we have calculated the band inversion strength (BIS) which is nothing but the energy difference between s-like Γ_6 and p-like Γ_8 state. The BIS is positive for trivial band order and negative for inverted band order. Figure 2(d) shows the variation of BIS (triangle down) with a change in hydrostatic strain. One can notice that with an expansion of only ∼0.35% (negative pressure of ∼11.9kbar) of the equilibrium lattice, a topological transition from trivial to nontrivial band insulator occurs. Under compression, the band gap (triangle up) slowly increases keeping the system a trivial band insulator.

2. Uniaxial strain

Half-Heusler materials with inverted band ordering are not naturally insulating because the two couples of bands with Γ symmetry are protected by the cubic symmetry and are degenerate at the Γ point. A way to break this degeneracy and open a band gap at the Γ point is to distort the cubic lattice by using proper uniaxial strain [19]. Figure 2(g) shows the variation of band gap vs the (c/a) ratio. The trivial

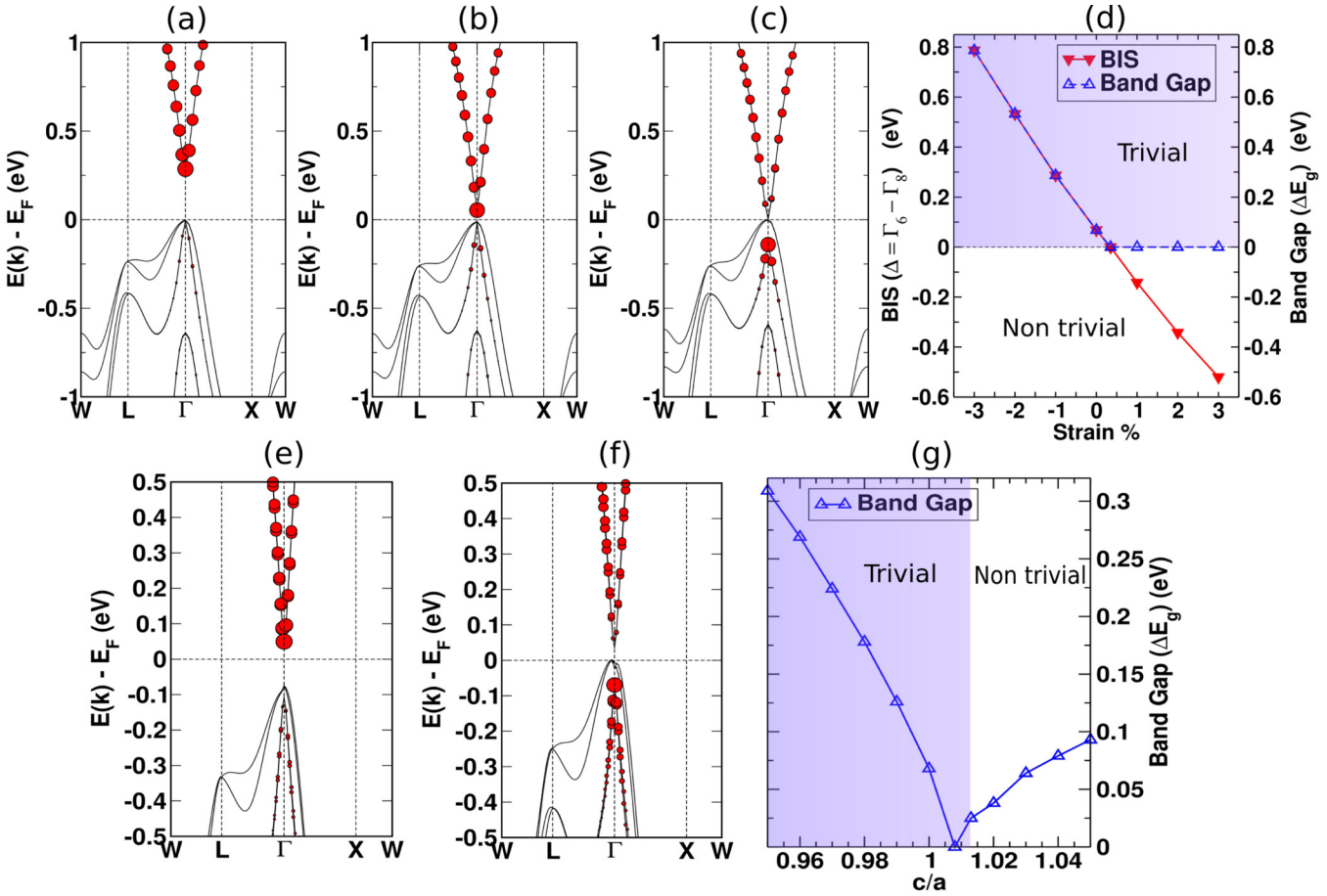

FIG. 2. Bulk band structure of ZrIrBi for cubic lattice at lattice constant (a) $a_{\text{opt}} - 1\% a_{\text{opt}}$, (b) a_{opt}, and (c) $a_{\text{opt}} + 1\% a_{\text{opt}}$, and uniaxially strained case (e) $c/a = 0.99$ and (f) $c/a = 1.02$. $a_{\text{opt}} = 6.48$ Å is the theoretically relaxed lattice parameter. Red dots denote the s-like orbitals. Size of the dots represents its weightage. Band inversion occurs in the expanded lattice case. (d) Band inversion strength (BIS) and band gap vs hydrostatic strain. (g) Band gap vs the uniaxial strain (c/a).

and nontrivial regions are clearly shown in the plot. Above $c/a = 1.013$ (1.13% stretch along [001] direction, equivalent to a negative pressure of ∼14.9kbar), band inversion occurs which sustain for larger strain. As the c/a ratio increases, the nontrivial band gap also increases. Due to the reduced crystal symmetry of the lattice, the degeneracy of the Γ_8 bands are lifted and thus the band gaps shown in Fig. 2(g) are not truly direct in nature. To illustrate further, we have plotted the full band structure for $c/a = 0.99$ and 1.02 in Figs. 2(e) and 2(f), respectively. This clearly shows the s/p band inversion at the Γ point for $c/a = 1.02$ but not for $c/a = 0.99$.

3. Alloy formation

Another possible way to achieve topological phase transition is alloying or doping the parent compound. We have investigated various combinations of alloying on each constituent site, i.e., Zr, Ir, and Bi. Out of these, two alloys show nontrivial band inversion. They are (i) arsenic (As) substitution at Bi site, i.e., $ZrIr(As_{0.5}Bi_{0.5})$ and (ii) hafnium (Hf) substitution at Zr site, i.e., $(Zr_{0.5}Hf_{0.5})$IrBi. The relaxed lattice parameter for the two cases are 6.33 and 6.47 Å, respectively. This is expected because As is relatively smaller than Bi, while Hf and Zr are of similar size. Figures 3(a) and 3(b) show the bulk band structure of $ZrIr(As_{0.5}Bi_{0.5})$ and $(Zr_{0.5}Hf_{0.5})$IrBi, respectively. Both compounds show gapless behavior. The p-like bands preserve the fourfold degeneracy at the Γ point, while the s-like states (labeled by red dots) lies, in energy, below the p-type states

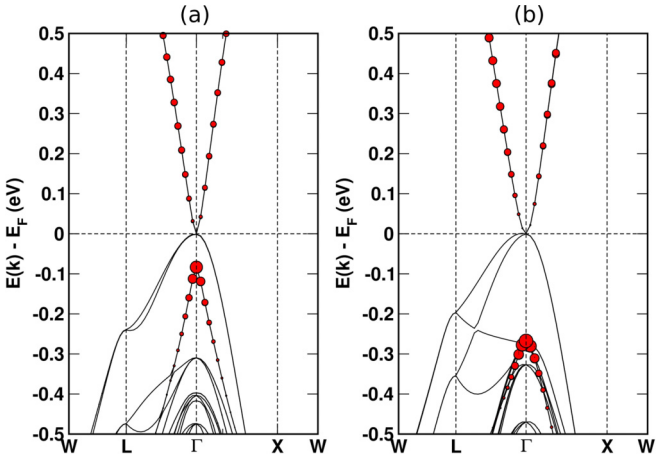

FIG. 3. Bulk band structure of (a) $ZrIr(As_{0.5}Bi_{0.5})$ and (b) $(Zr_{0.5}Hf_{0.5})$IrBi alloy at their theoretically relaxed lattice structure. Nontrivial band inversion is clearly observed.

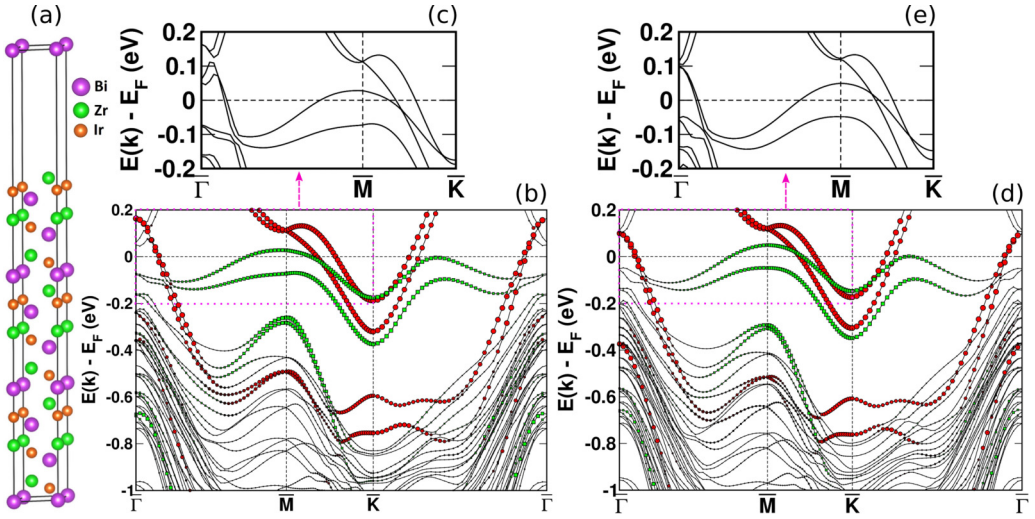

FIG. 4. (a) Unit cell for the (111) surface. Surface bands for ZrIrBi at (b) 1.0% hydrostatic expansion and (d) 2% uniaxial strain along the z axis. Red and green dots indicate the contributions of surface atoms from the bottom three (Bi-Ir-Zr) and top three (Ir-Bi-Zr) atomic layers, respectively. (c) and (e) The zoomed version of (b) and (d) along $\bar{\Gamma}$-$\bar{M}$-$\bar{K}$ line.

owing to the band inversion. Notably, although the lattice constant for As-substituted alloy is ∼2.5% smaller than the parent ZrIrBi compound, the former still shows nontrivial band inversion unlike ZrIrBi at a similar compressed lattice constant. This clearly indicates that arsenic plays a crucial role in band inversion, i.e., it is the chemical structure and not the geometrical volume which dictates nontriviality of the band structure in this case. The same argument goes for the Hf-substituted compound as well.

For a relatively more accurate estimate of the topological phase transition points, bulk calculations for all three cases are also done with a hybrid exchange correlation functional (HSE-06). A comparative result for HSE vs PBE is shown in the Supplemental Material [20].

C. Surface analysis

Surface bands are important to clarify the topological class of a material. Ternary half-Heusler compounds are layered structures along [111] direction and thus the most naturally cleavable surface is the (111) plane. We have constructed a surface slab along [111] direction for ZrIrBi with a_{opt} and 1% expanded lattice parameters. The slab geometry possess the hexagonal symmetry with the z axis pointed along [111] direction. The corresponding surface Brillouin zone (BZ) is shown in Fig. 1(c). A 27 atomic-layer thick slab with Bi and Zr termination at the bottom and top surface, respectively, is simulated for the surface electronic structure [see Fig. 4(a)]. This terminated surface is energetically the most favorable surface (as discussed in the Supplemental Material [20]). To neglect the coupling between the top and bottom surface, a vacuum of ∼13 Å is introduced. Atoms near the surfaces (5 atomic layers on each of the top and bottom sides) are fully relaxed in all the slab calculations converging the energy (force) up to 10^{-6} eV/cell (0.001 eV/Å). Maximum change in the internal z coordinate of atoms lie within 0.5%–1% depending on the atomic layer. Surface BZ integrations were done using $8 \times 8 \times 1$ Γ-centered k mesh.

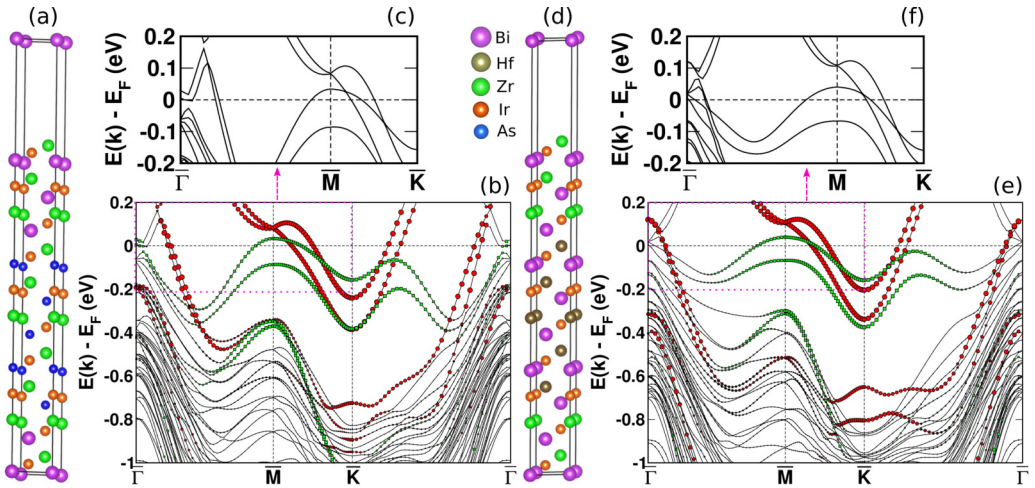

FIG. 5. (a) and (b) Slab unit cell and the surface band structure of ZrIr($As_{0.5}Bi_{0.5}$) along the (111) surface. (d) and (e) Same as (a) and (b), but for ($Zr_{0.5}Hf_{0.5}$)IrBi. (c) and (f) The zoomed version of (b) and (e) along $\bar{\Gamma}$-$\bar{M}$-$\bar{K}$ line.

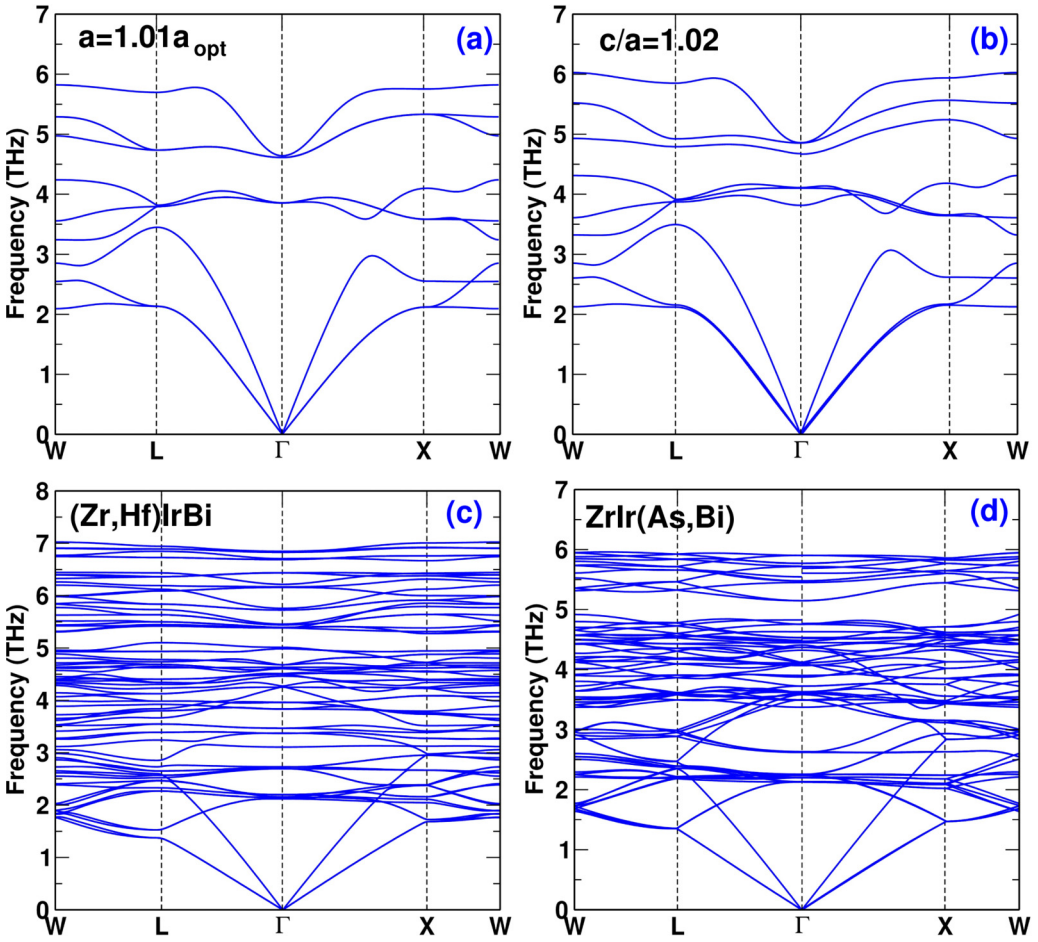

FIG. 6. Phonon dispersion for ZrIrBi with (a) hydrostatic expansion ($a = 1.01a_{\text{opt}}$), (b) uniaxial strain ($c/a = 1.02$), and the two alloys (c) $ZrIr(As_{0.5}Bi_{0.5})$ and (d) $(Zr_{0.5}Hf_{0.5})IrBi$.

Figure 4(b) shows the surface band structure of the topological nontrivial phase of ZrIrBi at the inflated lattice parameter ($1.01a_{\text{opt}}$). Red circles and green squares represent the contribution of surface atoms from the bottom three (Bi-Ir-Zr) and top three atomic layers (Zr-Ir-Bi), respectively. The most significant contribution actually comes from the first two consecutive layers from both ends of the slab. Contributions from other atomic layers (fourth layer onwards) are vanishingly small. Size of the symbols represent weightage of surface atoms contribution. Figure 4(c) shows a closer look of the surface bands along $\bar{\Gamma}$-$\bar{M}$-$\bar{K}$ direction. Notably, a pair of surface bands, arising from the bottom layer (Bi-Ir-Zr) of the slab, degenerately meet a little above E_F (~0.11 eV) at the $\bar{M}$ point. These bands dominantly reflect the Bi and Ir character. An exactly similar nature of bands is also observed in half-Heusler GdPtBi [21] which lie at/near E_F. In this case, a different energy position of these bands are due to the different constituent atoms contribution (Gd and Pt). Another interesting observation from Fig. 4(c) is the odd number (total 3) of Fermi crossings along the $\bar{\Gamma}$-$\bar{M}$ line segment which is directly consistent with the strong topological insulating phenomenon [22,23]. In contrast, an even number (total 6) of Fermi crossings were observed in GdPtBi.

In the uniaxially strained case ($c/a = 1.02$), a similar surface slab is constructed. Figure 4(d) shows the corresponding surface bands. Red circles and green squares indicate similar atomic contribution as in Fig. 4(b). Surface conduction in this case shows close resemblance to that of the hydrostatic expansion case. An odd number (3) of Fermi surface crossing is observed in this case as well, confirming the topological insulating phenomenon.

For the alloy case, a (111) surface slab is constructed for $ZrIr(As_{0.5}Bi_{0.5})$ and $(Zr_{0.5}Hf_{0.5})IrBi$ using the bulk relaxed lattice parameters. Figures 5(a) and 5(d) shows a 30 atomic-layer thick surface slab with As and Hf alloying, respectively. A vacuum of 11 Å is added in both cases, to nullify the interaction between the top and bottom surface. The site occupancy of the substitution element is important here. In Figs. 5(a) and 5(d) As and Hf are placed at the central layer (mostly acting like bulk) of the slab. We have varied the As and Hf positions across the layers, and observed the evolution in surface bands, which

TABLE I. Formation energies (in eV/atom) of ZrIrBi with hydrostatic expansion ($a = 1.01a_{\text{opt}}$), uniaxial strain ($c/a = 1.02$), and the two alloys $ZrIr(As_{0.5}Bi_{0.5})$ and $(Zr_{0.5}Hf_{0.5})IrBi$.

System	$a = 1.01a_{\text{opt}}$	$c/a = 1.02$	ZrIr(As,Bi)	(Zr,Hf)IrBi
ΔE_f	−0.596	−0.526	−0.731	−0.573

turn out to be similar. Figures 5(b) and 5(e) show the surface band structure for As and Hf substituted compounds. Surface states are metallic in nature in both cases. As in the previous case, red circles (green squares) indicate the contribution of surface atoms from the bottom three (top three) atomic layers. The nature of bands in the vicinity of $\bar{M}$ and $\bar{K}$ points looks similar in both alloy cases. Significant differences are observed near the $\bar{\Gamma}$ point, where the Hf-substituted alloy tends to show a Dirac-conelike feature a little above the E_F. On the other hand, As-substituted alloy shows almost flat band near E_F arising from the atoms at the bottom surface layers. An odd number of Fermi surface crossing along $\bar{\Gamma}$-$\bar{M}$ is observed in both alloys.

III. STABILITY

In order to investigate the possibilities of the experimental synthesis for the above newly proposed compounds, we have checked the chemical and mechanical (dynamical) stability of these compounds. Chemical stability is checked by calculating the formation energies using the formula $\Delta E_f = E_{\text{Comp}} - \sum_{i=1}^{n} x_i E_i$, where E_{Comp} is the total energy of the half-Heusler compounds and E_i represents the energy of the constituent elements in their equilibrium phase, all at their equilibrium lattice constants. x_i is the proportion of the ith element in the compound. Table I shows the formation energies of four potential candidates. Negative ΔE_f supports the chemically stability of these compounds.

We have also checked the dynamical stability by calculating the phonon dispersion, as shown in Fig. 6. Clearly, positive phonon frequencies in the entire k range confirms the dynamical stability of these compounds. If one closely analyzes the dispersion at/near the Γ point, it shows splitting between the longitudinal optical (LO) and transverse optical (TO) branches (commonly known as LO-TO splitting) indicating the existence of the ionic bonding in the crystal in all four cases. Such splitting in the strained cases are relatively smaller compared to those in the parent ZrIrBi compound. This is due to the relatively larger values of the components of static dielectric tensor in the former case (see the Supplemental Material [20] for more details).

In conclusion, we have shown that the half-Heusler compound ZrIrBi can be tuned to a new class of 3D topological insulator/semimetal via proper strain and substitution engineering. This is confirmed from first-principles calculation, by simulating both the bulk as well as surface band structure. Band inversion is realized by small hydrostatic and uniaxial expansion ($\leqslant 1.5\%$), as well as As and Hf substitution. Uniaxial strain gives rise to a topological insulating phase while the other two yields a topological semimetal phase. The possibility of experimental synthesis is confirmed by presenting the chemical and mechanical stability of all the compounds. Such *ab initio* predictions serve as a guiding path for the discovery of new novel materials.

ACKNOWLEDGMENTS

We thank L. Ke for helpful discussion. C.K.B. acknowledges IIT Bombay for financial support in the form of teaching assistantship. A.A. acknowledges National Center for Photovoltaic Research and Education (NCPRE), IIT Bombay for computational facilities.

[1] M. Z. Hasan and C. L. Kane, Colloquium: Topological insulators, Rev. Mod. Phys. **82**, 3045 (2010).
[2] X. Qi and S.-C. Zhang, Topological insulators and superconductors, Rev. Mod. Phys. **83**, 1057 (2011).
[3] J. E. Moore, The birth of topological insulators, Nature (London) **464**, 194 (2010).
[4] C. L. Kane and E. J. Mele, Z_2 Topological Order and the Quantum Spin Hall Effect, Phys. Rev. Lett. **95**, 146802 (2005).
[5] Y. Ando, Topological insulator materials, J. Phys. Soc. Jpn. **82**, 102001 (2013).
[6] L. Fu and C. L. Kane, Topological insulators with inversion symmetry, Phys. Rev. B **76**, 045302 (2007).
[7] D. Xiao, Y. Yao, W. Feng, J. Wen, W. Zhu, X.-Q. Chen, G. M. Stocks, and Z. Zhang, Half-Heusler Compounds as a New Class of Three-Dimensional Topological Insulators, Phys. Rev. Lett. **105**, 096404 (2010).
[8] W. Al-Sawai, H. Lin, R. S. Markiewicz, L. A. Wray, Y. Xia, S.-Y. Xu, M. Z. Hasan, and A. Bansil, Topological electronic structure in half-Heusler topological insulators, Phys. Rev. B **82**, 125208 (2010).
[9] S.-Y. Lin, M. Chen, X.-B. Yang, Y.-J. Zhao, S.-C. Wu, C. Felser, and B. Yan, Theoretical search for half-Heusler topological insulators, Phys. Rev. B **91**, 094107 (2015).
[10] D. Hsieh, D. Qian, L. Wray, Y. Xia, Y. S. Hor, R. J. Cava, and M. Z. Hasan, A topological Dirac insulator in a quantum spin Hall phase, Nature (London) **452**, 970 (2008).
[11] Y. Xia, D. Qian, D. Hsieh, L. Wray, A. Pal, H. Lin, A. Bansil, D. Grauer, Y. S. Hor, R. J. Cava, and M. Z. Hasan, Observation of a large-gap topological-insulator class with a single Dirac cone on the surface, Nat. Phys. **5**, 398 (2009).
[12] H. Zhang, C.-X. Liu, X.-L. Qi, X. Dai, Z. Fang, and S.-C. Zhang, Topological insulators in Bi_2Se_3, Bi_2Te_3 and Sb_2Te_3 with a single Dirac cone on the surface, Nat. Phys. **5**, 438 (2009).
[13] R. Gautier, X. Zhang, L. Hu, L. Yu, Y. Lin, T. O. L. Sunde, D. Chon, K. R. Poeppelmeier, and A. Zunger, Prediction and accelerated laboratory discovery of previously unknown 18-electron ABX compounds, Nat. Chem. **7**, 308 (2015).
[14] G. Kresse and J. Hafner, *Ab initio* molecular dynamics for liquid metals, Phys. Rev. B **47**, 558 (1993).
[15] G. Kresse and D. Joubert, From ultrasoft pseudopotentials to the projector augmented-wave method, Phys. Rev. B **59**, 1758 (1999).
[16] P. E. Blöchl, Projector augmented-wave method, Phys. Rev. B **50**, 17953 (1994).
[17] J. Heyd, G. E. Scuseria, and M. Ernzerhof, Hybrid functionals based on a screened Coulomb potential, J. Chem. Phys. **118**, 8207 (2003).

[18] B. A. Bernevig, T. L. Hughes, and S.-C. Zhang, Quantum spin Hall effect and topological phase transition in HgTe quantum wells, Science **314**, 1757 (2006).

[19] X. M. Zhang, W. H. Wang, E. K. Liu, G. D. Liu, Z. Y. Liu, and G. H. Wu, Influence of tetragonal distortion on the topological electronic structure of the half-Heusler compound LaPtBi from first principles, Appl. Phys. Lett. **99**, 071901 (2011).

[20] See Supplemental Material at http://link.aps.org/supplemental/10.1103/PhysRevB.97.075302 for detailed theoretical results using hybrid exchange correlation functional (HSE06) and the surface band structures for various terminating surfaces.

[21] C. Liu, Y. Lee, T. Kondo, E. D. Mun, M. Caudle, B. N. Harmon, S. L. Bud'ko, P. C. Canfield, and A. Kaminski, Metallic surface electronic state in half-Heusler compounds RPtBi (R = Lu, Dy, Gd), Phys. Rev. B **83**, 205133 (2011).

[22] H. Lin, L. A. Wray, Y. Xia, S. Xu, S. Jia, R. J. Cava, A. Bansil, and M. Zahid Hasan, Half-Heusler ternary compounds as new multi-functional experimental platforms for topological quantum phenomena, Nat. Mater. **9**, 546 (2010).

[23] S. Chadov, X. Qi, J. Kübler, G. H. Fecher, C. Felser, and S. C. Zhang, Tunable multi-functional topological insulators in ternary Heusler compounds, Nat. Mater. **9**, 541 (2010).